



RESEARCH

Open Access



Plasma cell-free DNA methylation profile before afatinib treatment is associated with progression-free and overall survival of patients with epidermal growth factor receptor gene mutation-positive non-small cell lung cancer

Mao Fujimoto^{1†}, Hiroyuki Yasuda^{2†}, Eri Arai^{1*} , Makoto Nakajima¹, Saori Takata³, Kei Morikawa⁴, Hisashi Tanaka⁵, Hidetoshi Itani⁶, Takeshi Honda⁷, Kazuya Horiuchi⁸, Kageaki Watanabe⁹, Hideyuki Nakagawa¹⁰, Yoshiro Nakahara¹¹, Yoshitaka Seki¹², Akihiro Bessho¹³, Nobumasa Takahashi¹⁴, Kentaro Hayashi¹⁵, Takeo Endo¹⁶, Kiyoshi Takeyama¹⁷, Toshiya Maekura¹⁸, Nagio Takigawa¹⁹, Akikazu Kawase²⁰, Makoto Endoh²¹, Kenji Nemoto²², Kazuma Kishi²³, Kenzo Soejima²⁴, Yusuke Okuma⁹, Akira Togashi²⁵, Noriyuki Matsutani²⁶, Nobuhiko Seki⁷ and Yae Kanai^{1*} 

Abstract

Background The present study aimed to clarify the clinical significance of the cell-free DNA (cfDNA) methylation profile of patients with non-small cell lung cancer (NSCLC) showing the *epidermal growth factor receptor* (EGFR) gene mutation.

Methods In 103 patients, genome-wide DNA methylation analysis using Infinium Methylation EPIC array was performed using samples of pre-tyrosine kinase inhibitor afatinib-treatment plasma cfDNA (n = 101) and post-afatinib cfDNA (n = 84).

Results Principal component analysis indicated that the cfDNA methylation profile was altered after afatinib treatment. Hierarchical clustering using the pre-afatinib cfDNA methylation profile revealed that cases with a fatal outcome were accumulated in specific clusters. Moreover, Kaplan–Meier analysis showed that the pre-afatinib cfDNA methylation profile was significantly associated with both progression-free survival (PFS) and overall survival (OS), whereas the post-afatinib profile was not. The genes for which pre-afatinib cfDNA methylation levels were associated with PFS were accumulated in the cadherin, Wnt, and EGFR signaling pathways. Activation of EGFR-related signaling

[†]Mao Fujimoto and Hiroyuki Yasuda have contributed equally to this work.

*Correspondence:

Eri Arai
earai@keio.jp
Yae Kanai
ykanai@keio.jp

Full list of author information is available at the end of the article



© The Author(s) 2025. **Open Access** This article is licensed under a Creative Commons Attribution-NonCommercial-NoDerivatives 4.0 International License, which permits any non-commercial use, sharing, distribution and reproduction in any medium or format, as long as you give appropriate credit to the original author(s) and the source, provide a link to the Creative Commons licence, and indicate if you modified the licensed material. You do not have permission under this licence to share adapted material derived from this article or parts of it. The images or other third party material in this article are included in the article's Creative Commons licence, unless indicated otherwise in a credit line to the material. If material is not included in the article's Creative Commons licence and your intended use is not permitted by statutory regulation or exceeds the permitted use, you will need to obtain permission directly from the copyright holder. To view a copy of this licence, visit <http://creativecommons.org/licenses/by-nc-nd/4.0/>.

due to DNA methylation alterations might overturn the effect of afatinib. Pre-afatinib levels of *CEP170* and *CHCHD6* cfDNA methylation were associated with both PFS and OS. Both pre- and post-afatinib cfDNA methylation levels of *SLC9A3R2* and *INTS1* were associated with bone metastasis. Using the cfDNA methylation levels at two CpG sites, cg12721600 and cg05905155, patients showing an overall response were predicted with a sensitivity of 96% or more.

Conclusions The non-invasively measurable cfDNA methylation profile may reflect the corresponding profile in cancer cells, and that pre-treatment measurement may provide clinically useful information on EGFR mutation-positive NSCLC.

Keywords Cell-free DNA, DNA methylation, Lung adenocarcinoma, Epidermal growth factor receptor, Afatinib

Background

It is widely acknowledged that epigenomic alterations are pivotal in the process of carcinogenesis in multiple human organs [1, 2]. Aberrant DNA methylation is considered to be one of the most significant epigenomic changes, contributing to chromosomal instability and expression alteration of cancer-related genes [3]. In the context of non-small cell lung cancer (NSCLC), many groups have reported the results of genome-wide DNA methylation analysis using clinical tissue samples [4–6]. For instance, we have demonstrated that DNA methylation profiles corresponding to background factors of carcinogenesis, e.g. smoking and chronic obstructive lung disease, are already established in the precancer stage [7–10]. As is also the case in cancers of other organs [11–13], DNA methylation profiles at the precancer stage are inherited by or strengthened in pathological specimens of NSCLC itself, thus determining the clinicopathological aggressiveness and patient outcome [7–9]. Therefore, monitoring of DNA methylation profiles non-invasively and repeatedly using blood samples would offer many clinical advantages.

Cell-free DNA (cfDNA) is defined as a mixture of nucleic acids released into the bloodstream primarily through the processes of apoptosis and necrosis of circulating cells [14]. While the concentration of cfDNA in healthy adults is typically negligible, levels in cancer patients have been documented to reach up to 50 times higher [15]. Consequently, a proportion of the cfDNA may be attributable to the apoptosis and necrosis of circulating tumour cells. It is acknowledged that genetic and epigenetic status obtained from cfDNA molecules can be considered as a reflection of such status of the tumor cells [16, 17]. Although DNA methylation status based on cfDNA samples has already been assessed in NSCLC patients [18–21], the correlation between the cfDNA methylation profile and the clinicopathological diversity of NSCLCs has not yet been fully examined in a large number of patients. In the present study, to clarify

the clinical significance of cfDNA methylation profiles, genome-wide analysis was performed using cfDNA samples from pre- and post-treatment pair blood samples of 103 NSCLC patients after collection of detailed clinical information.

Methods

Patients and methods

A total of 103 patients, with a median age of 70 years (ranging from 42 to 88 years), histopathologically diagnosed with metastatic or locally advanced NSCLC, were collected between February 2017 and March 2018 at 21 hospitals in Japan [22]. The majority of patients (90%) exhibited common EGFR mutations, i.e. exon 19 deletions and exon 21 L858R substitutions, while the remaining 10% demonstrated rare EGFR mutations. All patients had an Eastern Cooperative Oncology Group performance status [23] of 0 or 1, indicating adequate bone marrow, renal, and liver functions, and being chemotherapy-naïve. The patients were divided into an initial cohort (n=60) and a validation cohort (n=43) depending on whether they were enrolled in the first or second half of the study period. Characteristics of patients in both cohorts are summarized in Table 1.

Patients who had been enrolled were initially treated with 40 mg/day afatinib, a second-generation irreversible tyrosine kinase inhibitor [24], and the dose was adjusted according to observed toxicities [22]. According to the Response Evaluation Criteria in Solid Tumors, version 1.1 [25], tumor response was assessed until progressive disease (PD), treatment discontinuation, withdrawal of consent, or death. The overall response rate and disease control rate were 60.2% (95% confidence interval [CI]: 50.1–69.7) and 87.4% (95% CI: 79.4–93.1), respectively. The median progression-free survival (PFS) was 18.4 months, while the median overall survival (OS) was not reached. This study complied with the Declaration of Helsinki and was approved by the Ethics Committees at Keio University School of Medicine (Approval No. 2021–0147) and at Teikyo University (Approval No. 16–066). All enrolled patients provided written informed consent.

Table 1 Clinicopathological characteristics of the initial and validation cohorts of the patients with non-small cell lung cancer

Clinicopathological parameters	Number of patients or median (range)		<i>P</i> ^d
	Initial cohort (n = 60)	Second cohort (n = 43)	
Age (years)	70 (42–86)	73 (50–88)	0.145
Less than 70	29	21	1.00
70 or more	31	22	
Sex			
Male	12	15	0.164
Female	48	28	
Histological type			
Adenocarcinoma	60	43	
EGFR mutation			
Exon 19 deletion	34	18	0.315
Exon 21 L858R	21	20	
Others	5	5	
Exon 18	2	1	
Exon 20 insertion	1	2	
Exon 20 T790M	0	1	
Exon 21 L861Q	1	0	
Exon 20 S768I + Exon 18 G719X	1	1	
Performance status ^a			
0	26	26	0.111
1	34	17	
Lymph node metastasis ^b			
Negative	51	38	0.351
Positive	9	3	
Bone metastasis ^b			
Negative	57	37	0.437
Positive	3	4	
Stage			
III and IV	44	31	1.00
Post-surgical recurrence positive	16	12	
Response ^c			
Complete response	3	1	0.812
Partial response	34	24	
Stable disease	16	11	
Progressive disease	2	0	
Not applicable	5	5	

^a According to the eastern cooperative oncology group performance status [23]^b Only patients for whom a diagnosis regarding metastasis to each organ has been made are described^c According to the response evaluation criteria in solid tumors, version 1.1 [25]^d Welch's t-test for age (years) and Fisher's exact-test for all other parameters

Infinium assay

Pre-afatinib blood samples were collected from 101 patients immediately prior to oral administration, while

post-afatinib blood samples were obtained from 84 patients 8 weeks \pm 7 days after the commencement of administration. Five milliliters of plasma was subjected to cfDNA extraction using a QIAamp Circulating Nucleic Acid Kit (Qiagen, Hilden, Germany). We performed bisulfite conversion using the total amount of extracted cfDNA minus that required for genomic analysis with an EZ DNA Methylation-Gold Kit (Zymo Research, Irvine, CA, USA). The DNA methylation status at 865,918 probe loci was examined using the Infinium MethylationEPIC BeadChip (Illumina, San Diego, CA, USA) [26]. Following hybridization, the hybridized DNA was fluorescence-labeled by a single-base extension reaction and then detected by an iScan Reader (Illumina). GenomeStudio Methylation software (Illumina) was used for the initial quality control. At each CpG site, β -values were computed as DNA methylation levels (0.00 to 1.00) defined as the signal intensity of the methylated probe relative to the summed signal intensity of the methylated and unmethylated probes.

The call proportions (detection *P* values < 0.01) for 29,065 probes in all 185 samples were less than 90%. Given that such a low proportion may have been attributable to polymorphism in these participants, these probes were filtered out, as previously described [27, 28]. Furthermore, 17,274 probes containing more than 10% missing β -values were excluded. Consequently, 2932 probes designed for non-CpG loci and 59 designed for detection of single-nucleotide polymorphisms were also excluded. In order to avoid any gender-specific methylation bias, the 19,627 probes on chromosomes X and Y were also filtered out, leaving a final total of 815,746 probe CpG sites for further analysis.

Statistics

DNA methylation profiles of pre- and post-afatinib cfDNA samples were subjected to principal component analysis. Hierarchical clustering (Manhattan distances, Ward's method) was performed using the cfDNA methylation profiles. Kaplan–Meier curves were generated for DNA hyper- and hypo-methylation groups at each CpG site. Differences of PFS and OS between the DNA hyper- and hypo-methylation groups were examined by log-rank test. Pathway analysis using genes showing significant correlations with PFS and OS was performed using the protein analysis through evolutionary relationships (PANTHER) database (version 18.0, <https://www.pantherdb.org>). Correlations between cfDNA methylation profiles and metastasis were examined by Welch's t-test. Correlations between DNA methylation and transcription levels were examined using the Clinical Proteomic Tumor Analysis Consortium (CPTAC) database (dbGaP Study Accession: phs001287, <https://proteomics.cancer>).

[gov/programs/cptac](https://cancer.gov/programs/cptac)). For each CpG site, a receiver operating characteristic (ROC) curve was generated to discriminate patients showing overall response (OR) to afatinib. The Youden index was defined as a cutoff value for OR prediction. $P < 0.05$ was considered to indicate statistical significance, and multiple testing correction was performed by calculating q -values. All statistical analyses were performed using the R software package (R Foundation for Statistical Computing) (<https://www.r-project.org>).

Results

DNA methylation profile of cfDNA samples from NSCLC patients

To overview the DNA methylation profiles of 101 pre-afatinib cfDNA samples and 84 post-afatinib cfDNA samples from among the 103 patients (both the initial and validation cohorts), principal component analysis was performed using the DNA methylation levels at the 815,746 probe CpG sites (Fig. 1A). The pre-afatinib samples are scattered over a wide area on the scatterplot, whereas the post-afatinib samples showed clustering in a smaller area of the plot, suggesting that afatinib treatment had altered the cfDNA methylation profile. The wide dispersal of the pre-afatinib samples on the scatterplot (Fig. 1A) may have reflected the clinicopathological diversity of the tumors prior to modification by the treatment.

To further clarify the clinical impact of the pre-afatinib cfDNA methylation profile, hierarchical clustering (Manhattan distances, Ward's method) was performed for the 101 patients from whom pre-afatinib blood samples were obtained (both cohorts) (Fig. 1B). Fatal outcomes were accumulated in Clusters I and IIA (43 in total; 62.8%) relative to Cluster IIB (58 in total; 24.1%) ($P = 1.85 \times 10^{-4}$, Fisher's exact test), suggesting that the pre-afatinib cfDNA methylation profile was associated with patient outcome after treatment. Hierarchical clustering using the post-afatinib cfDNA methylation levels revealed no such accumulation of fatal cases into certain clusters.

Correlation between pre-afatinib cfDNA methylation profile and PFS

For all the 815,746 probe CpG sites, median values of the pre-afatinib cfDNA methylation levels in the initial cohort ($n = 60$) were defined as the cutoff values dividing the DNA hypermethylation and hypomethylation groups. Kaplan–Meier curves for PFS were generated for these sites and examined using Log-rank test. At 1785 CpG sites, significant differences of PFS were observed between the DNA hypermethylation and hypomethylation groups in the initial cohort ($P < 0.05$, $q < 0.3$): DNA hypermethylation at 1212 CpG sites and DNA

hypomethylation at 573 CpG sites were associated with unfavorable PFS. Kaplan–Meier curves for PFS in the initial cohort for the top 5 CpG sites with the smallest P -values are shown in Fig. 2A.

Similarly, patients in the validation cohort ($n = 41$) were divided into DNA hypermethylation and hypomethylation groups using the same cutoff values defined in the initial cohort. At 251 of the 1785 CpG sites, significant differences of PFS between these groups were validated in the validation cohort ($P < 0.05$, $q < 0.3$) and the direction of alteration (DNA hypermethylation or hypomethylation in the unfavorable group relative to the favorable group) was also matched in both cohorts: DNA hypermethylation at 186 CpG sites and DNA hypomethylation at 65 CpG sites were associated with unfavorable PFS. Supplemental Table S1 summarizes chromosomal position, gene names, annotation and CpG types for all of the 251 CpG sites. Annotation refers to the distinction between TSS1500 (from 200 bp upstream of the transcription start site [TSS] to 1500 bp upstream of it), TSS200 (from the TSS to 200 bp upstream of it), the 5' untranslated region (UTR), 1st exon, gene body (1st intron and downstream), the 3'UTR and the intergenic region, identified using the RefSeq database (<http://www.ncbi.nlm.nih.gov/refseq/>). CpG types refer to the distinction between CpG islands, island shores and island shelves, identified using the University of California, Santa Cruz database (<https://genome.ucsc.edu/>). Kaplan–Meier curves in the validation cohort are shown in Fig. 2B. On the other hand, using the post-afatinib cfDNA methylation levels, no CpG site showed significant correlations with PFS in either of the cohorts.

Using the 232 genes for which the 251 probes were designed, pathway over-representation analysis was performed on pathways with 50–500 component genes from the PANTHER database. Over-representation of the 232 genes was observed in 7 pathways ($P < 0.05$ and false discovery rate [FDR] < 0.1), including the cadherin signaling pathway ($P = 2.06 \times 10^{-4}$ and $\text{FDR} = 2.43 \times 10^{-3}$), Wnt signaling pathway ($P = 2.21 \times 10^{-4}$ and $\text{FDR} = 2.43 \times 10^{-3}$) and EGFR signaling pathway ($P = 2.05 \times 10^{-3}$ and $\text{FDR} = 1.51 \times 10^{-2}$) (Table 2).

Since over-representation was observed in the EGFR signaling pathway, we examined correlations between EGFR mutation patterns (exon 19 deletion, exon 21 L858R and others [exon 18, exon 20 insertion, exon 20 T790M, exon 21 L861Q, exon 20 S768I + exon 18 G719X]) and pre- and post-afatinib cfDNA methylation status. Hierarchical clustering (Manhattan distances, Ward's method) for the 101 patients from whom pre-afatinib blood samples were obtained and that for the 84 patients from whom post-afatinib blood samples were obtained revealed no significant accumulation of specific

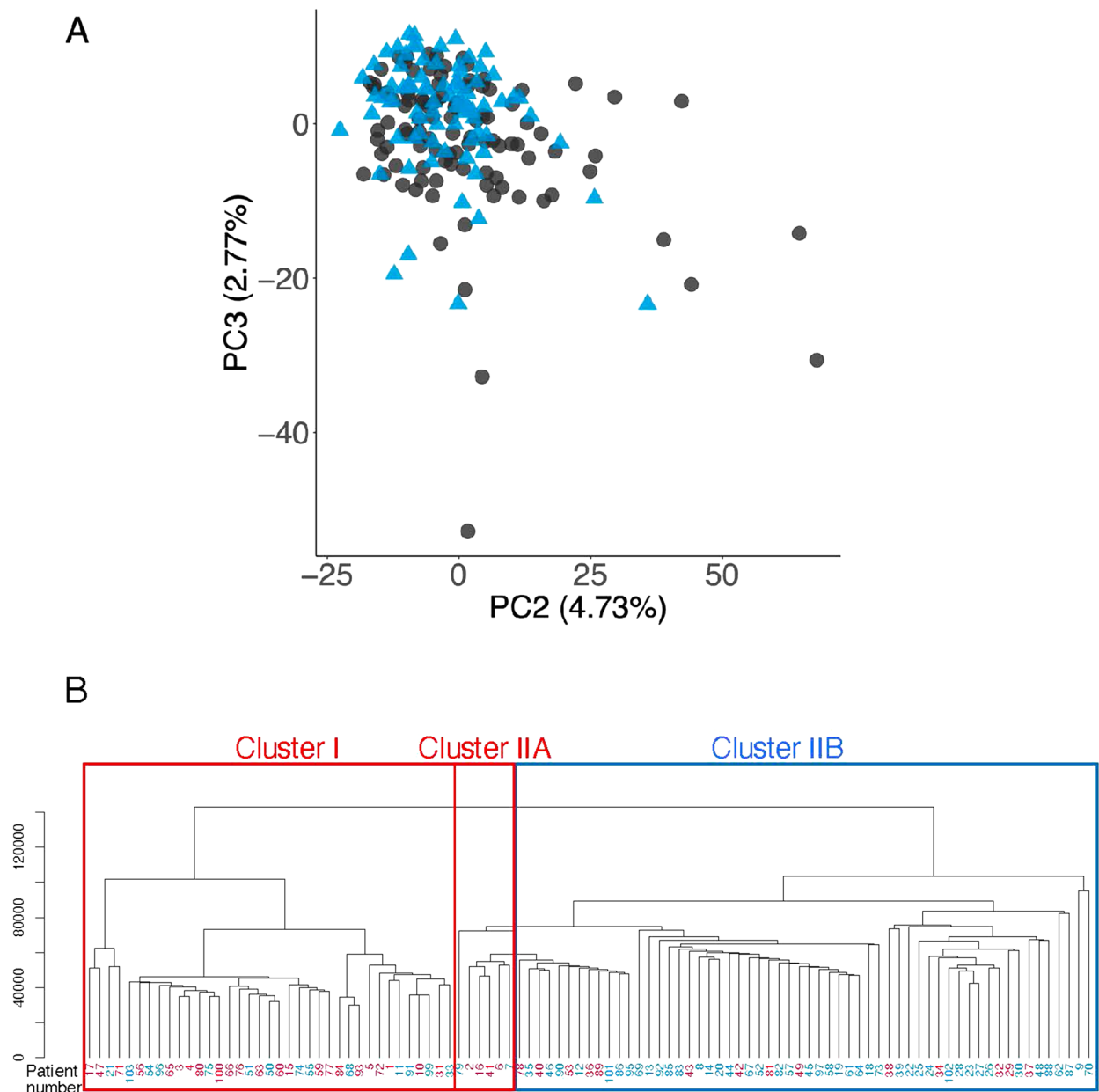


Fig. 1 Cell-free DNA (cfDNA) methylation profiles of non-small cell lung cancer patients. **A** Principal component (PC) analysis of 101 pre-afatinib cfDNA samples (black circles) and 84 post-afatinib cfDNA samples (blue triangles) from among 103 patients using the DNA methylation levels of all of the 815,746 probe CpG sites. The pre-afatinib samples are scattered over a wide area on the scatterplot, whereas the post-afatinib samples appear clustered in a smaller area, suggesting that the cfDNA methylation profile tended to be altered by afatinib treatment. **B** Hierarchical clustering (Manhattan distances, Ward's method) in the 101 patients from whom pre-afatinib blood samples were obtained. Patients who survived and who died are shown in blue and red, respectively, at the bottom of the dendrogram. Fatal cases are accumulated in Clusters I and IIA ($n=43$; 62.8%) relative to Cluster IIB ($n=58$; 24.1%) ($P=1.85 \times 10^{-4}$, Fisher's exact test)

(See figure on next page.)

Fig. 2 Correlations between pre-afatinib cell-free DNA (cfDNA) methylation profile and progression-free survival (PFS) in patients with non-small cell lung cancer. Patients belonging to the initial cohort ($n=60$) **A** and the validation cohort ($n=41$) **B** are divided into a DNA hypermethylation group (Hyper) and a DNA hypomethylation group (Hypo) using the median values of the pre-afatinib cfDNA methylation levels in the initial cohort as the cutoff values (CV). Kaplan–Meier curves for PFS at 5 CpG sites showing the smallest P -values in the initial cohort using Log-rank test are shown. The Infinium assay probe ID for each CpG site and gene symbol are shown on the left side of each Kaplan–Meier curve

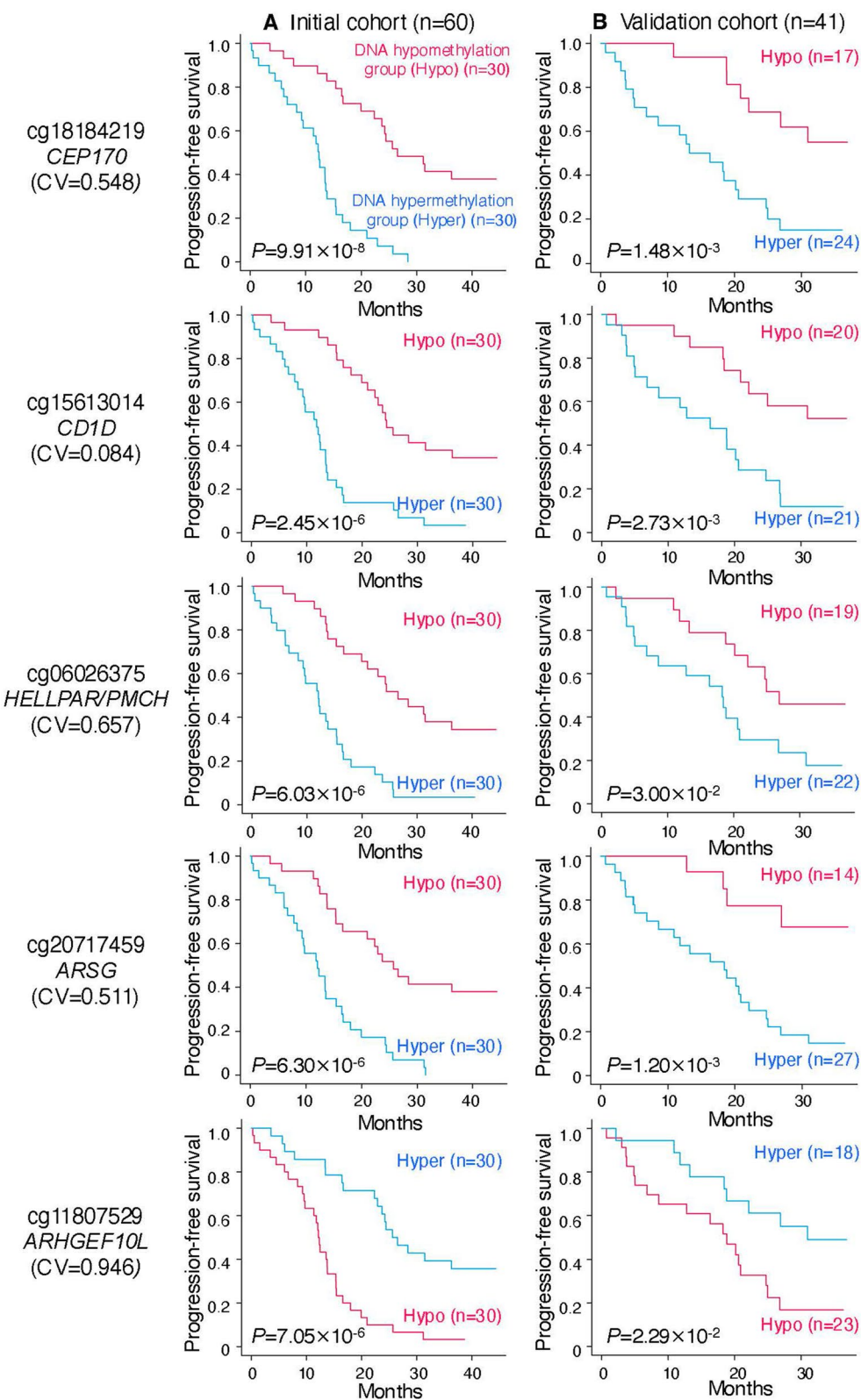


Fig. 2 (See legend on previous page.)

Table 2 Pathway over-representation analysis using the 232 genes for which the 251 probes showing pre-afatinib cell-free DNA (cfDNA) methylation profiles correlated with progression-free survival (PFS) are designed, based on the protein analysis using the evolutionary relationships database (version 18.0, <https://www.pantherdb.org>) ($P < 0.05$ and false discovery rate [FDR] < 0.1)

ID	Description	P	FDR	Genes for which cfDNA methylation status was correlated with PFS and are involved in the pathway
P00012	Cadherin signaling pathway	2.06×10^{-4}	2.43×10^{-3}	<i>PCDHGA2, PCDHGB2, PCDHGA1, PCDHGB1, CDH6, CTNNA2, PCDHGA5, PCDHGA3</i>
P00057	Wnt signaling pathway	2.21×10^{-4}	2.43×10^{-3}	<i>PCDHGA2, PCDHGB2, PCDHGA1, PCDHGB1, CDH6, NKD2, CTNNA2, SMARCA2, PLCB4, PCDHGA5, PCDHGA3</i>
P00018	EGF receptor signaling pathway	2.05×10^{-3}	1.51×10^{-2}	<i>PIK3C2A, PIK3R6, CCM2, PLCB4, TGFA, PHLDB2</i>
P00019	Endothelin signaling pathway	1.05×10^{-2}	5.76×10^{-2}	<i>PRKG1, PIK3C2A, PIK3R6, PLCB4</i>
P00060	Ubiquitin proteasome pathway	1.91×10^{-2}	7.33×10^{-2}	<i>PSMD6, WWP1, UBE2H</i>
P04391	Oxytocin receptor mediated signaling pathway	2.00×10^{-2}	7.33×10^{-2}	<i>PLCB4, CACNA1C, CACNA1D</i>
P04374	5HT2 type receptor mediated signaling pathway	2.78×10^{-2}	8.75×10^{-2}	<i>PLCB4, CACNA1C, CACNA1D</i>

mutation pattern into certain clusters (data not shown). In addition, correlations between EGFR mutation patterns and pre- and post-afatinib cfDNA methylation levels of the genes – *PIK3C2A*, *PIK3R6*, *CCM2*, *PLCB4*, *TGFA* and *PHLDB2* – involved in the EGFR signaling pathway in Table 2 are shown in Supplemental Fig. S1. Although NSCLCs with “others” ($n = 10$) showed lower cfDNA methylation levels of the *PIK3C2A* gene in their pre-afatinib samples and lower cfDNA methylation levels of the *PIK3R6* and *PLCB4* genes in their post-afatinib samples, in general, no clear correlations between EGFR mutation patterns and cfDNA methylation profiles were observed before and after treatment (Supplemental Fig. S1).

Correlation between pre-afatinib cfDNA methylation profile and OS

For all 815,746 probe CpG sites, Kaplan–Meier curves for OS were generated for the DNA hypermethylation and hypomethylation groups based on the median pre-afatinib cfDNA methylation levels in the initial cohort as the cutoff values. At 60 CpG sites, significant differences of OS between the two groups were observed in both the initial and validation cohorts ($P < 0.05$, $q < 0.3$) and the direction of alteration (DNA hypermethylation or hypomethylation in the unfavorable group relative to the favorable group) was also matched in both cohorts: DNA hypermethylation at 51 CpG sites and DNA hypomethylation at 9 CpG sites were associated with unfavorable

OS. Chromosomal position, gene names, annotation and CpG types for all of the 60 CpG sites are summarized in Supplemental Table S2. Kaplan–Meier curves for both cohorts are shown in Fig. 3. On the other hand, using the post-afatinib cfDNA methylation levels, no CpG site showed significant correlations with OS in either cohort.

Although pathway over-representation analysis was performed using the PANTHER database using the 72 genes for which the 60 probes were designed, no significant over-representation was observed in any pathway ($P < 0.05$ and $FDR < 0.1$). On the other hand, DNA hypermethylation of the *CEP170*, *CHCHD6*, *HELLPAR*, *PMCH*, *AC079921.1*, *KLHL5*, *TYW1B*, *LAMA4* and *TRH* genes was revealed to be significantly correlated with both poorer PFS and OS ($P < 0.05$, $q < 0.3$) in both cohorts (Supplemental Table S3).

Correlation between cfDNA methylation profile and metastasis of NSCLCs

Next, we speculated that even the post-afatinib cfDNA methylation profile might be associated with metastases after treatment. On the other hand, as afatinib was also administered to patients who had already developed metastases, correlations between both post-afatinib and pre-afatinib cfDNA methylation profiles and metastases were examined. Significant differences of post-afatinib DNA methylation levels at the 361 CpG sites were observed between patients positive ($n = 7$) and negative ($n = 44$) for lymph node metastasis

(See figure on next page.)

Fig. 3 Correlation between the pre-afatinib cell-free DNA (cfDNA) methylation profile and overall survival (OS) in patients with non-small cell lung cancer. Patients belonging to the initial cohort ($n = 60$) **A** and the validation cohort ($n = 41$) **B** are divided into a DNA hypermethylation group (Hyper) and a DNA hypomethylation group (Hypo) using the median values of the pre-afatinib cfDNA methylation levels in the initial cohort as the cutoff values (CV). Kaplan–Meier curves for OS at 5 CpG sites showing the smallest P -values in the initial cohort using Log-rank test are shown. The Infinium assay probe ID for each CpG site and gene symbol are shown on the left side of each Kaplan–Meier curve

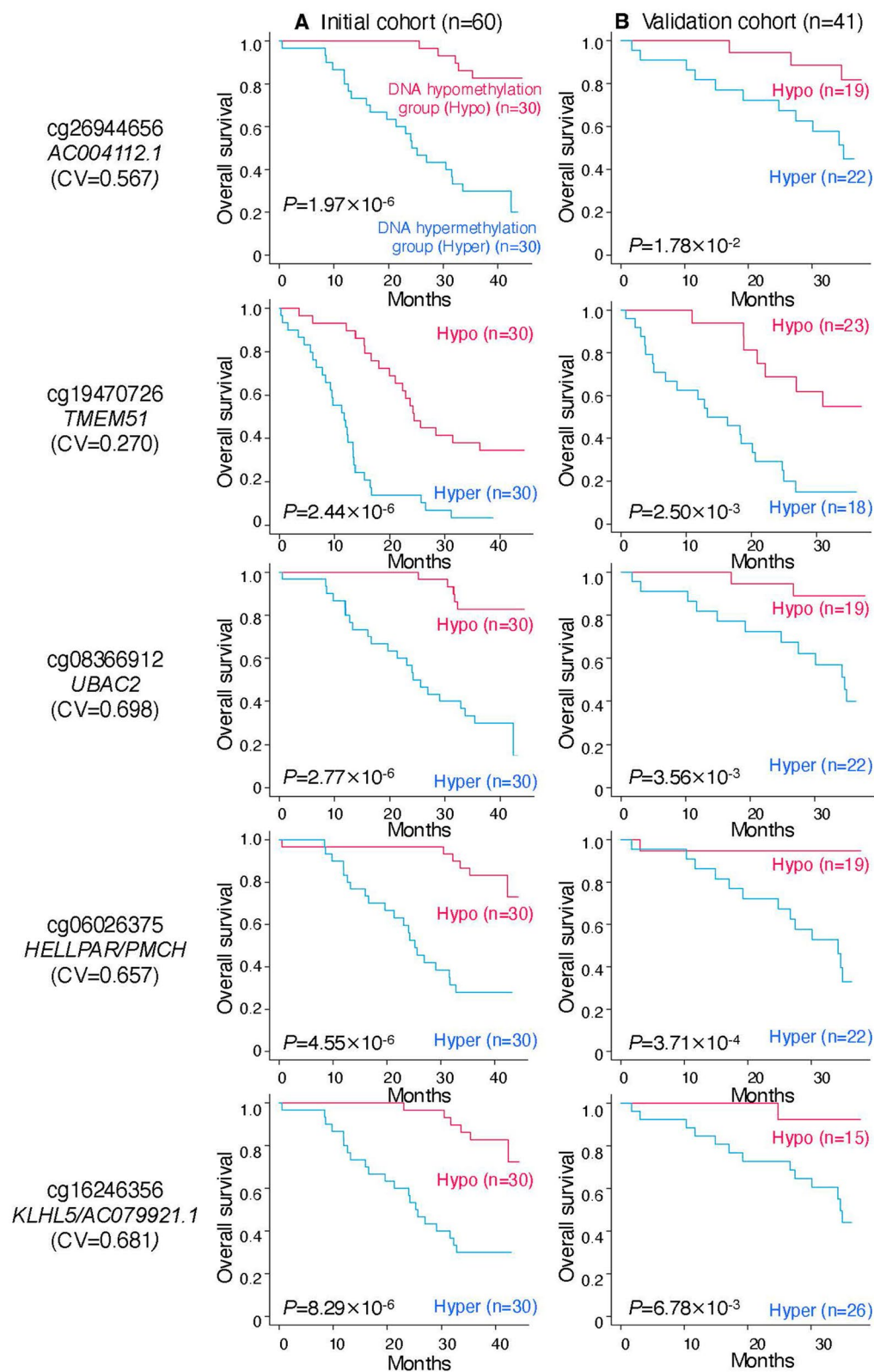


Fig. 3 (See legend on previous page.)

in the initial cohort ($P < 0.05$, $q < 0.3$ and $\Delta\beta_{\text{positive-negative}} > 0.1$ or < -0.1). At 23 of the 361 CpG sites, significant differences between lymph node metastasis-positive ($n = 3$) and -negative ($n = 30$) patients were validated in the validation cohort. Similarly, significant differences of pre-afatinib DNA methylation levels at the 8 CpG sites were observed between lymph node metastasis-positive and -negative patients in both the initial and validation cohorts ($P < 0.05$, $q < 0.3$ and $\Delta\beta_{\text{positive-negative}} > 0.1$ or < -0.1). Both post-afatinib and pre-afatinib cfDNA methylation levels at one CpG site were significantly correlated with lymph node metastasis in both cohorts (Supplemental Table S4A).

Similarly, both post-afatinib and pre-afatinib cfDNA methylation levels at the 16 CpG sites were significantly correlated ($P < 0.05$, $q < 0.3$ and $\Delta\beta_{\text{positive-negative}} > 0.1$ or < -0.1) with bone metastasis in both the initial cohort ($n = 3$ and $n = 57$ in positive and negative patients, respectively) and the validation cohort ($n = 4$ and $n = 37$, respectively) (Supplemental Table S4B).

Correlations between DNA methylation and transcription levels of genes whose cfDNA methylation levels had clinical impacts on NSCLC patients

DNA methylation alterations of cancer cells may contribute to clinicopathological characteristics such as PFS, OS and metastasis, presumably via stable alterations in transcription levels. Therefore, correlations between DNA methylation levels and transcription levels of 47 genes, i.e. the 22 genes in Table 2 (correlated with PFS and accumulated in cancer-related signaling pathways), 8 genes in Supplemental Table S3 (correlated with both PFS and OS) and 17 genes in Supplemental Table S4 (correlated with lymph node or bone metastasis), were examined using data for 482 samples of human tissue from various organs deposited in the CPTAC database. Data for the *PMCH* gene in Supplemental Table S3 were not deposited in the CPTAC database. For 14 of the 47 genes, i.e. the *NKD2*, *CCM2*, *PIK3R6*, *SMARCA2*, *PCDHGB1*, *PLCB4*, *PIK3C2A* and *CACNA1D* genes in Table 2, the *CEP170* and *CHCHD6* genes in Supplemental Table S3, and the *SLC9A3R2*, *INTS1*, *PRXL2A* and *AC008073.3* genes in Supplemental Table S4, significant inverse or positive correlations between DNA methylation and transcription levels were confirmed ($P < 0.05$ and $r > 0.2$ or < -0.2) (Supplemental Fig. S2).

Prediction of response to afatinib in NSCLC patients based on their cfDNA methylation profiles

In an attempt to give some clinical relevance to our data, for all of the 815,746 probe CpG sites, ROC curves

were generated for OR (complete response and partial response) using the pre-afatinib cfDNA methylation levels for the 60 patients in the initial cohort, 53 of whom showed OR. AUC values of more than 0.9 were observed at 114 CpG sites, for which the Youden index was defined as the cutoff value. For 2 of the 114 CpG sites, both sensitivity and specificity for discrimination of patients showing OR were more than 70% in both cohorts (Table 3). For example, the sensitivity and specificity for OR prediction of cg12721600 were 79% and 100% in the initial cohort and 72% and 80% in the validation cohort, respectively. For prediction of OR when one or two of the CpG sites of cg12721600 and cg05905155 met those criteria, the sensitivity was 96% and 97% in the initial and validation cohorts, respectively (Table 3).

Discussion

The fact that the pre-afatinib samples were widely dispersed on the PCA scatterplot (Fig. 1A) may at least partly reflect the diversity of the clinicopathological characteristics of the patients prior to modification resulting from treatment. In fact, hierarchical clustering using the pre-afatinib cfDNA methylation data yielded specific clusters of fatal cases. Moreover, pre-afatinib cfDNA methylation levels at specific CpG sites were significantly correlated with both PFS and OS. No such clustering or correlation was observed in the post-afatinib cfDNA methylation data, suggesting that cfDNA methylation profiles can be altered by treatment. It is plausible that response to treatment is to some extent defined by the DNA methylation profile of cancer cells before treatment. Furthermore, it would be of clinical value if the behavior of cancer cells after treatment could be predicted by assessment of cfDNA methylation profiles before treatment.

The marked differences in survival between the DNA hyper- and hypo-methylation groups, divided simply on the basis of the median cfDNA methylation levels as the cutoff, were surprising. In particular, the genes whose cfDNA methylation levels were correlated with PFS were accumulated in the cadherin and Wnt molecular pathways. The cadherin pathway is an important tumor-suppressive pathway involved in cell adhesion, and hence cell proliferation, invasion and metastasis [29], while the Wnt pathway is an important oncogenic pathway [30]. In addition, transmembrane cadherins interact with the Wnt system by tethering β -catenin molecules to the plasma membrane [29]. We can consider that DNA methylation alterations of the genes involved in these two pathways lead to clinically recognizable disease progression through crosstalk between the cadherin and Wnt pathways.

Table 3 Prediction of overall response (OR) to afatinib based on cfDNA methylation levels at two marker CpG sites that each individually showed a sensitivity and specificity of over 70% in the initial and validation cohorts

Infinium probe ID	Chr	Position ^a	Gene symbol	Annotation ^b	CpG type ^c	Cutoff value ^d	DNA methylation status ^e	Initial cohort (n = 60) ^f		Validation cohort (n = 41) ^g	
								Sensitivity ^h (%)	Specificity ⁱ (%)	Sensitivity ^h (%)	Specificity ⁱ (%)
cg12721600	Chr1	34,862,186	NA	Intergenic region	S Shelf/N Shelf	0.843	Hypo	79	100	72	80
cg05905155	Chr16	30,802,803	NA	Intergenic region	N Shelf	0.672	Hyper	72	100	78	80
One or two of cg12721600 and cg05905155 satisfying above criteria								96	100	97	60

Chr, chromosome; AUC, area under the curve; NA, not applicable

^a Chromosomal coordinates are based on the genome assembly GRCh38 (<https://www.ncbi.nlm.nih.gov/grc/human>)

^b Annotations were identified based on the RefSeq database (<https://www.ncbi.nlm.nih.gov/refseq/>); transcription start site (TSS) 1500 (200–1500 bases upstream of the TSS), TSS200 (0–200 bases upstream of the TSS), 5' untranslated region (UTR), 1st exon, gene body (1st intron and downstream), 3'UTR and intergenic region

^c CpG types were identified on the basis of the University of California Santa Cruz database (<https://genome.ucsc.edu>); CpG islands, island shores (2000-bp regions adjacent to a CpG island) and island shelves (2000-bp regions adjacent to an island shore). N and S indicate upstream and downstream from islands, respectively

^d The Youden index was defined as the cutoff value

^e Hypo, cfDNA methylation levels of patients showing OR are expected to be lower than the cutoff values; Hyper, cfDNA methylation levels of patients showing OR are expected to be higher than the cutoff values

^f Fifty-three of 60 patients showed OR in the initial cohort

^g Thirty of 41 patients showed OR in the validation cohort

^h Sensitivity is defined as the ratio of the number of patients predicted to respond to afatinib based on our criteria relative to the exact number of patients showing OR

ⁱ Specificity is defined as the ratio of the number of patients not predicted to respond to afatinib based on our criteria relative to the exact number of patients not showing OR

Interestingly, the genes whose cfDNA methylation levels correlated with PFS are also accumulated in the EGFR molecular pathway. Among the 4 genes involved in the EGFR pathway in Table 2 and Supplemental Fig. S2 (*CCM2*, *PIK3R6*, *PLCB4* and *PIK3C2A*), in particular, an inverse correlation between DNA methylation and transcription levels for *CCM2* and *PIK3R6* was clear on the scatterplots (Supplemental Fig. S2). *CCM2* acts as a scaffold for assembly of the RAC GTPase and the MAPK kinase kinase MEKK3, and *CCM2* silencing reportedly activates MAPK activity [31, 32]. It is understandable that when *CCM2* expression is reduced in the DNA hypermethylation group, MAPK would be activated, resulting in increased cancer cell growth and disease progression. On the other hand, *PIK3R6* is a regulatory subunit of PI3K γ , and *PIK3R6* silencing induces apoptosis and reduces human cancer cell invasion [33]. Indeed, overexpression of *PIK3R6* has been reported in ovarian cancer [33] and renal cell carcinoma [34]. It is also understandable that NSCLCs in the DNA hypomethylation group would have shown disease progression, possibly via overexpression of *PIK3R6*. Activation of EGFR-related signaling due to DNA methylation alterations might overturn the EGFR inhibitory effect of afatinib. It may make sense to monitor the DNA methylation levels of EGFR signal-related molecules using cfDNA samples to estimate the response to afatinib in patients showing EGFR mutations. In general, since clear correlations were not observed between EGFR mutation patterns, exon 19 deletion, exon 21 L858R and others, and cfDNA methylation profiles (Supplemental Fig. S1), reduction of the effect of afatinib through DNA methylation abnormalities may not depend on the specific mutation pattern.

Furthermore, *CEP170* and *CHCHD6* were identified as genes for which cfDNA methylation levels were consistently correlated with PFS to OS. In the unfavorable PFS and OS groups, cfDNA hypermethylation of *CEP170* may have reflected its reduced expression in cancer cells. The centrosomal component CEP170 plays a role in microtubule formation and reportedly contributes to the development of cancers with copy number alterations [35]. Overexpression of CEP170 has been reported in patients with pancreatic cancers showing poor prognosis [36]. On the other hand, CEP170 is important for activating the DNA damage response [37], and cancers showing low levels of CEP170 may be responsive to DNA-damaging agents. Therefore, administration of such agents might be applicable to PD cases after afatinib treatment.

In the unfavorable PFS and OS groups, cfDNA hypermethylation of *CHCHD6* may have reflected its overexpression, since a positive correlation between the DNA methylation level at the CpG site and its transcription

level was confirmed in a database (Supplemental Fig. S2). *CHCHD6* participates in the maintenance of cristae, and indispensable for mitochondrial function [38]. Although the relationship between *CHCHD6* and cancer has not been well studied to date, *CHCHD6* deficiency reportedly impairs cell proliferation [39]. Therefore, it is not surprising that *CHCHD6* is highly expressed in cancers with poorer PFS and OS.

Among the genes that were associated with lymph node and bone metastases, inverse or positive correlations between DNA methylation and transcription levels for *SLC9A3R2*, *INTS1*, *PRXL2A* and *AC008073.3* were confirmed using the CPTAC database. Moreover, the scattergrams in Supplemental Fig. S2 suggested that *PRXL2A* and *AC008073.3* might also be regulated by mechanisms other than DNA methylation, whereas an inverse correlation between DNA methylation and the transcription level of *SLC9A3R2* and a positive correlation for *INTS1* were clear on the scattergrams. *SLC9A3R2* regulates *SLC9A3*, a sodium/hydrogen exchanger in the brush-border membrane participating in transepithelial sodium absorption [40]. cfDNA hypermethylation of the *SLC9A3R2* gene has been reported in a previous study of lung cancer patients [20], being consistent with the present results. More interestingly, DNA hypermethylation and reduced expression have been reported in samples of portal vein tumor thrombi from patients with hepatocellular carcinoma relative to both primary hepatocellular carcinoma tissue and non-cancerous liver tissue samples [41]. NSCLC generally metastasizes to bone via vascular invasion. By analogy with the findings for portal vein thrombi [41], NSCLCs may acquire DNA hypermethylation in the vasculature, resulting in decreased expression in bone metastasis-positive cases. On the other hand, *INTS1* is one of the subunits of the integrator complex and plays an important role in the regulation of RNA polymerase II-dependent genes [42]. Overexpression of *INTS1* has been reported in hepatocellular [42] and gastric [43] carcinomas. It is not surprising that DNA hypermethylation of *INTS1*, possibly resulting in its overexpression, was found in NSCLC patients with metastases.

Finally, we attempted to create a diagnostic criterion to predict the responsiveness of cancer cells to afatinib prior to treatment. Combination of cfDNA methylation levels at two marker CpG sites that each individually showed a sensitivity and specificity of over 70% in both cohorts was able to predict OR with a sensitivity of 96% or more. The CpG sites under scrutiny were found to be located within intergenic regions, rather than in the vicinity of the TSS of specific genes. This finding is consistent with the results of our previous studies showing that alterations in DNA methylation at CpG sites not involved in

regulating the expression of functionally important genes can serve as effective surrogate markers for diagnostic purposes [44, 45]. Even though it is desirable to improve specificity by screening of a larger cohort, the present results suggest that cfDNA methylation levels can be a biomarker for prediction of response to molecular targeting therapies.

Conclusions

DNA methylation abnormalities in the cadherin- and Wnt-signaling pathways may play a role in unfavorable PFS. DNA methylation abnormalities in the EGFR pathway-related genes might reduce the effect of afatinib. Pretreatment cfDNA methylation abnormalities of *CEP170* and *CHCHD6* were correlated with both PFS and OS, and pre- and post-treatment cfDNA methylation abnormalities of *SLC9A3R2* and *INTS1* were correlated with metastasis of NSCLC. cfDNA methylation levels of specific CpG sites before treatment may be applicable for use as markers to predict response to afatinib. These findings suggest that evaluation of cfDNA methylation profiles in patients with EGFR mutation-positive NSCLC may be useful for understanding tumor aggressiveness and patient outcome.

Abbreviations

AUC	Area under the curve
cfDNA	Cell-free DNA
CI	Confidence interval
CPTAC	Clinical proteomic tumor analysis consortium
EGFR	Epidermal growth factor receptor
FDR	False discovery rate
NSCLC	Non-small cell lung cancer
OR	Overall response
OS	Overall survival
PANTHER	Protein analysis through evolutionary relationships
PD	Progressive disease
PFS	Progression-free survival
ROC	Receiver operating characteristic
TSS	Transcription start site
UTR	Untranslated region

Supplementary Information

The online version contains supplementary material available at <https://doi.org/10.1186/s13148-025-01870-8>.

Additional file 1.

Author contributions

MF: Methodology, Software, Formal analysis, Investigation, Data Curation, Writing—Original Draft, Visualization. HY: Methodology, Validation, Resources, Writing—Review & Editing, Visualization. EA: Methodology, Software, Validation, Formal analysis, Investigation, Data Curation, Writing—Original Draft, Visualization, Supervision. MN: Software, Formal analysis, Investigation, Data Curation, Writing—Original Draft, Visualization. ST, KM, HT, HI, TH, KH (Kazuya Horiuchi), KW, HN, YN, YS, AB, NT, KH (Kentarō Hayashi), TE, KT, TM, NT, AK, ME, KN, KK, KS and YO: Resources, Writing—Review & Editing. AT: Conceptualization, Funding acquisition. NM: Conceptualization, Resources, Project administration, Writing—Review & Editing. NS: Conceptualization, Resources, Project administration, Funding acquisition, Writing—Review & Editing. YK:

Conceptualization, Methodology, Formal analysis, Investigation, Data Curation, Writing—Original Draft, Visualization, Supervision, Project administration, Funding acquisition.

Funding

This work was supported by Nippon Boehringer Ingelheim Co., Ltd., Tokyo, Japan (S01PA84234).

Availability of data and materials

The results of the Infinium assay have been deposited in the Gene Expression Omnibus (<https://www.ncbi.nlm.nih.gov/geo/>) database (Accession number: GSE277078). This study is the methylome component of the exosome-focused translational research for afatinib (EXTRA) study [22]. The EXTRA study aimed to identify novel biomarkers via multi-omics analyses and was registered with the University Hospital Medical Information Network clinical trial registry (No. UMIN000024935).

Declarations

Ethics approval and consent to participate

This study complied with the Declaration of Helsinki and was approved by the Ethics Committee at Keio University School of Medicine (2021–0147) and the Ethical Review Board for Medical and Health Research Involving Human Subjects at Teikyo University (16–066). All participants provided written informed consent.

Competing interests

AT is an employee of Nippon Boehringer Ingelheim Co., Ltd., Tokyo, Japan.

Author details

¹Department of Pathology, Keio University School of Medicine, 35 Shinanomachi, Shinjuku-Ku, Tokyo 160-8582, Japan. ²Division of Pulmonary Medicine, Department of Medicine, Keio University School of Medicine, Tokyo, Japan. ³Department of Respiratory Medicine, Kyorin University School of Medicine, Tokyo, Japan. ⁴Division of Respiratory Medicine, Department of Internal Medicine, St. Marianna University School of Medicine, Kawasaki, Japan. ⁵Department of Respiratory Medicine, Hirosaki University Graduate School of Medicine, Aomori, Japan. ⁶Department of Respiratory Medicine, Ise Red Cross Hospital, Ise, Mie, Japan. ⁷Division of Medical Oncology, Department of Internal Medicine, Teikyo University School of Medicine, Tokyo, Japan. ⁸Respiratory Disease Center, Showa University Northern Yokohama Hospital, Yokohama, Kanagawa, Japan. ⁹Department of Thoracic Oncology and Respiratory Medicine, Tokyo Metropolitan Cancer and Infectious Diseases Center, Komagome Hospital, Tokyo, Japan. ¹⁰Department of Respiratory Medicine, National Hospital Organization Hirosaki Hospital, Aomori, Japan. ¹¹Department of Respiratory Medicine, Kitasato University School of Medicine, Sagami-hara, Japan. ¹²Department of Internal Medicine, The Jikei University Daisan Hospital, Tokyo, Japan. ¹³Department of Respiratory Medicine, Japanese Red Cross Okayama Hospital, Okayama, Japan. ¹⁴Department of General Thoracic Surgery, Saitama Cardiovascular and Respiratory Center, Saitama, Japan. ¹⁵Division of Respiratory Medicine, Department of Internal Medicine, Nihon University School of Medicine, Tokyo, Japan. ¹⁶Department of Respiratory Medicine, National Hospital Organization Mito Medical Center, Higashiibaraki, Ibaraki, Japan. ¹⁷Department of Respiratory Medicine, Tokyo Women's Medical University School of Medicine, Tokyo, Japan. ¹⁸Department of Respiratory Medicine, Hoshigaoka Medical Center, Osaka, Japan. ¹⁹Department of General Internal Medicine 4, Kawasaki Medical School, Okayama, Japan. ²⁰First Department of Surgery, Hamamatsu University School of Medicine, Shizuoka, Japan. ²¹Department of Thoracic Surgery, Yamagata Prefectural Central Hospital, Yamagata, Japan. ²²Department of Respiratory Medicine, National Hospital Organization, Ibarakihigashi National Hospital, Naka, Ibaraki, Japan. ²³Department of Respiratory Medicine, Respiratory Center, Toranomon Hospital, Tokyo, Japan. ²⁴Clinical and Translational Research Center, Keio University Hospital, Tokyo, Japan. ²⁵Nippon Boehringer Ingelheim Co., Ltd., Tokyo, Japan. ²⁶Department of Surgery, Teikyo University Hospital, Mizonokuchi, Kanagawa, Japan.

Received: 21 January 2025 Accepted: 31 March 2025

Published online: 25 April 2025

References

- Jones PA, Issa J-P, Baylin S. Targeting the cancer epigenome for therapy. *Nat Rev Genet.* 2016;17:630–41.
- Baylin SB, Jones PA. Epigenetic determinants of cancer. *Cold Spring Harb Perspect Biol.* 2016;8: a019505.
- Kanai Y. Molecular pathological approach to cancer epigenomics and its clinical application. *Pathol Int.* 2024;74:167–86.
- Ito Y, Usui G, Seki M, Fukuyo M, Matsusaka K, Hoshii T, et al. Association of frequent hypermethylation with high grade histological subtype in lung adenocarcinoma. *Cancer Sci.* 2023;114:3003–13.
- Boyer L, Noguera-Uclés JF, Castillo-Peña A, Salinas A, Sánchez-Gastaldo A, Alonso M, et al. Aberrant methylation of the imprinted C19MC and MIR371-3 clusters in patients with non-small cell lung cancer. *Cancers (Basel).* 2023;15:1466.
- Yu F, Huang X, Zhou D, Zhao Z, Wu F, Qian B, et al. Genetic, DNA methylation, and immune profile discrepancies between early-stage single primary lung cancer and synchronous multiple primary lung cancer. *Clin Epigenetics.* 2023;15:4.
- Hamada K, Tian Y, Fujimoto M, Takahashi Y, Kohno T, Tsuta K, et al. DNA hypermethylation of the ZNF132 gene participates in the clinicopathological aggressiveness of 'pan-negative'-type lung adenocarcinomas. *Carcinogenesis.* 2021;42:169–79.
- Sato T, Arai E, Kohno T, Takahashi Y, Miyata S, Tsuta K, et al. Epigenetic clustering of lung adenocarcinomas based on DNA methylation profiles in adjacent lung tissue: Its correlation with smoking history and chronic obstructive pulmonary disease. *Int J Cancer.* 2014;135:319–34.
- Sato T, Arai E, Kohno T, Tsuta K, Watanabe S-i, Soejima K, et al. DNA methylation profiles at precancerous stages associated with recurrence of lung adenocarcinoma. *PLoS ONE.* 2013;8:e59444.
- Eguchi K, Kanai Y, Kobayashi K, Hirohashi S. DNA hypermethylation at the D17S5 locus in non-small cell lung cancers: its association with smoking history. *Cancer Res.* 1997;57:4913–5.
- Yang M, Arai E, Takahashi Y, Totsuka H, Chiku S, Taniguchi H, et al. Cooperative participation of epigenomic and genomic alterations in the clinicopathological diversity of gastric adenocarcinomas: significance of cell adhesion and epithelial-mesenchymal transition-related signaling pathways. *Carcinogenesis.* 2020;41:1473–84.
- Tsumura K, Arai E, Tian Y, Shibuya A, Nishihara H, Yotani T, et al. Establishment of permutation for cancer risk estimation in the urothelium based on genome-wide DNA methylation analysis. *Carcinogenesis.* 2019;40:1308–19.
- Kuramoto J, Arai E, Tian Y, Funahashi N, Hiramoto M, Nammo T, et al. Genome-wide DNA methylation analysis during non-alcoholic steatohepatitis-related multistage hepatocarcinogenesis: comparison with hepatitis virus-related carcinogenesis. *Carcinogenesis.* 2017;38:261–70.
- Thierry AR, Messaoudi SE, Gahan PB, Anker P, Stroun M. Origins, structures, and functions of circulating DNA in oncology. *Cancer Metastasis Rev.* 2016;35:347–76.
- Nikanjam M, Kato S, Kurzrock R. Liquid biopsy: current technology and clinical applications. *J Hematol Oncol.* 2022;15:131.
- Song P, Wu LR, Yan YH, Zhang JX, Chu T, Kwong LN, et al. Limitations and opportunities of technologies for the analysis of cell-free DNA in cancer diagnostics. *Nat Biomed Eng.* 2022;6:232–45.
- Luo H, Wei W, Ye Z, Zheng J, Xu R-H. Liquid biopsy of methylation biomarkers in cell-free DNA. *Trends Mol Med.* 2021;27:482–500.
- Nguyen TH, Doan NNT, Tran TH, Huynh LAK, Doan PL, Nguyen THH, et al. Tissue of origin detection for cancer tumor using low-depth cfDNA samples through combination of tumor-specific methylation atlas and genome-wide methylation density in graph convolutional neural networks. *J Transl Med.* 2024;22:618.
- Liang W, Zhao Y, Huang W, Gao Y, Xu W, Tao J, et al. Non-invasive diagnosis of early-stage lung cancer using high-throughput targeted DNA methylation sequencing of circulating tumor DNA (ctDNA). *Theranostics.* 2019;9:2056–70.
- Xu W, Lu J, Zhao Q, Wu J, Sun J, Han B, et al. Genome-wide plasma cell-free DNA methylation profiling identifies potential biomarkers for lung cancer. *Dis Markers.* 2019;2019:4108474.
- Hulbert A, Jusue-Torres I, Stark A, Chen C, Rodgers K, Lee B, et al. Early detection of lung cancer using DNA promoter hypermethylation in plasma and sputum. *Clin Cancer Res.* 2017;23:1998–2005.
- Takata S, Morikawa K, Tanaka H, Itani H, Ishihara M, Horiuchi K, et al. Prospective exosome-focused translational research for afatinib (EXTRA) study of patients with nonsmall cell lung cancer harboring EGFR mutation: an observational clinical study. *Ther Adv Med Oncol.* 2023;15:17588359231177020.
- Oken MM, Creech RH, Tormey DC, Horton J, Davis TE, McFadden ET, et al. Toxicity and response criteria of the Eastern cooperative oncology group. *Am J Clin Oncol.* 1982;5:649–55.
- Hurwitz JL, Scullin P, Campbell L. Afatinib treatment in advanced non-small cell lung cancer. *Lung Cancer.* 2011;247–57.
- Eisenhauer EA, Therasse P, Bogaerts J, Schwartz LH, Sargent D, Ford R, et al. New response evaluation criteria in solid tumours: revised RECIST guideline (version 1.1). *Eur J Cancer.* 2009;45:228–47.
- Bibikova M, Le J, Barnes B, Saedinia-Melnyk S, Zhou L, Shen R, et al. Genome-wide DNA methylation profiling using Infinium® assay. *Epigenomics.* 2009;1:177–200.
- Tsumura K, Fujimoto M, Tian Y, Kawahara T, Fujimoto H, Maeshima AM, et al. Aberrant cell adhesiveness due to DNA hypermethylation of KLF11 in papillary urothelial carcinomas. *Exp Mol Pathol.* 2024;137: 104908.
- Makiuchi S, Tian Y, Fujimoto M, Kuramoto J, Tsuda N, Ojima H, et al. DNA methylation alterations of ADCY5, MICAL2, and PLEKHG2 during the developmental stage of cryptogenic hepatocellular carcinoma. *Hepatol Res.* 2024;54:284–99.
- Hirohashi S, Kanai Y. Cell adhesion system and human cancer morphogenesis. *Cancer Sci.* 2003;94:575–81.
- Reya T, Clevers H. Wnt signalling in stem cells and cancer. *Nature.* 2005;434:843–50.
- Zhu Y, Wu Q, Xu JF, Miller D, Sandalcioğlu IE, Zhang J-M, et al. Differential angiogenesis function of CCM2 and CCM3 in cerebral cavernous malformations. *Neurosurg Focus.* 2010;29:E1.
- Chapman EM, Lant B, Ohashi Y, Yu B, Schertzberg M, Go C, et al. A conserved CCM complex promotes apoptosis non-autonomously by regulating zinc homeostasis. *Nat Commun.* 2019;10:1791.
- Liu YJ, Cui LL, Liu ZS, Jia R-Y, Ding Y-X, Xu L-Z, et al. RBBP6 aggravates the progression of ovarian cancer by targeting PIK3R6. *Eur Rev Med Pharmacol Sci.* 2020;24:10366–74.
- Yang J, Zhong X, Gao X, Xie W, Chen Y, Liao Y, et al. Knockdown of PIK3R6 impedes the onset and advancement of clear cell renal cell carcinoma. *Cell Adh Migr.* 2024;18:1–12.
- Xu X, Wang K, Vera O, Verma A, Jasani N, Bok I, et al. Gain of chromosome 1q perturbs a competitive endogenous RNA network to promote melanoma metastasis. *Cancer Res.* 2022;82:3016–31.
- Giordano G, Cipolletta G, Mellone A, Puopolo G, Coppola L, Santis ED, et al. Altered centriolar cohesion by CEP250 and appendages impact outcome of patients with pancreatic cancer. *Pancreatol.* 2024;24:899–908.
- Rodríguez-Real G, Domínguez-Calvo A, Prados-Carvajal R, Bayona-Feliú A, Gomes-Pereira S, Balestraet FR, et al. Centriolar subdistal appendages promote double-strand break repair through homologous recombination. *EMBO Rep.* 2023;24: e56724.
- Ding C, Wu Z, Huang L, Wang Y, Xue J, Chen S, et al. Mitofilin and CHCHD6 physically interact with Sam50 to sustain cristae structure. *Sci Rep.* 2015;5:16064.
- An J, Shi J, He Q, Lui K, Liu Y, Huang Y, et al. CHCM1/CHCHD6, novel mitochondrial protein linked to regulation of mitofilin and mitochondrial cristae morphology. *J Biol Chem.* 2012;287:7411–26.
- Yang J, Singh V, Cha B, Chen T-E, Sarker R, Murtazina R, et al. NHERF2 protein mobility rate is determined by a unique C-terminal domain that is also necessary for its regulation of NHE3 protein in OK cells. *J Biol Chem.* 2013;288:16960–74.
- Fan X, Li Y, Yi X, Chen G, Jin S, Dai Y, et al. Epigenome-wide DNA methylation profiling of portal vein tumor thrombosis (PVTT) tissues in hepatocellular carcinoma patients. *Neoplasia.* 2020;22:630–43.
- Xu Y, Liao W, Wang T, Zhang L, Zhang H. Comprehensive bioinformatics analysis of integrator complex subunits: expression patterns, immune infiltration, and prognostic signature, validated through experimental approaches in hepatocellular carcinoma. *Discov Oncol.* 2024;15:246.
- Wang H, Li NS, He C, Xie C, Zhu Y, Lu N-H, et al. Discovery and validation of novel methylation markers in *Helicobacter pylori*-associated gastric cancer. *Dis Markers.* 2021;2021:4391133.

44. Endo Y, Fujimoto M, Ito N, Takahashi Y, Kitago M, Gotoh M, et al. Clinicopathological impacts of DNA methylation alterations on pancreatic ductal adenocarcinoma: prediction of early recurrence based on genome-wide DNA methylation profiling. *J Cancer Res Clin Oncol*. 2021;147:1341–4.
45. Fujimoto M, Arai E, Tsumura K, Yotani T, Yamada Y, Takahashi Y, et al. Establishment of diagnostic criteria for upper urinary tract urothelial carcinoma based on genome-wide DNA methylation analysis. *Epigenetics*. 2020;15:1289–301.

Publisher's Note

Springer Nature remains neutral with regard to jurisdictional claims in published maps and institutional affiliations.